Enhanced ferroelectricity and ferromagnetism in $Bi_{0.9}Ba_{0.1}FeO_3/La_{2/3}Sr_{1/3}MnO_3$ heterostructure grown by pulsed laser deposition*

Wen Xiao-Li(温晓莉)[a], Chen Zhao(陈 钊)[b]†, Lin Xin(林 鑫)[a]‡, Niu Li-Wei(牛利伟)[b], Duan Meng-Meng(段萌萌)[b], Zhang Yun-Jie(张云婕)[b], Dong Xiang-Lei(董祥雷)[b], and Chen Chang-Le(陈长乐)[b]

[a] *State Key Laboratory of Solidification Processing, Northwestern Polytechnical University, Xi'an* 710072, *China*
[b] *Key Laboratory of Space Applied Physics and Chemistry of Ministry of Education, School of Science, Northwestern Polytechnical University, Xi'an* 710072, *China*

(Received 26 January 2014; revised manuscript received 27 March 2014; published online 24 September 2014)

$Bi_{0.9}Ba_{0.1}FeO_3$ (BBFO)/$La_{2/3}Sr_{1/3}MnO_3$ (LSMO) heterostructures are fabricated on $LaAlO_3$ (100) substrates by pulsed laser deposition. Giant remnant polarization value ($\sim$ 85 $\mu C/cm^2$) and large saturated magnetization value ($\sim$ 12.4 emu/cm^3) for BBFO/LSMO heterostructures are demonstrated at room temperature. Mixed ferroelectric domain structures and low leakage current are observed and in favor of enhanced ferroelectric properties in the BBFO/LSMO heterostructures. The magnetic field-dependent magnetization measurements reveal the enhancement in the magnetic moment and improved magnetic hysteresis loop originating from the BBFO/LSMO interface. The heterostructure is proved to be effective in enhancing the ferroelectric and ferromagnetic performances in multiferroic BFO films at room temperature.

Keywords: ferroelectric properties, ferromagnetic properties, $Bi_{0.9}Ba_{0.1}FeO_3/La_{2/3}Sr_{1/3}MnO_3$ heterostructures, interface coupling effect

PACS: 77.80.bn, 77.80.Dj, 75.70.Cn, 68.37.–d **DOI:** 10.1088/1674-1056/23/11/117703

1. Introduction

Multiferroic materials exhibit spontaneous polarization and magnetization simultaneously, and have attracted considerable attention because of their potential applications in multifunctional devices as well as interesting physics.[1–4] $BiFeO_3$ (BFO) is the most studied multiferroic compound because currently it is the only single-phase multiferroic material that has a giant remanent polarization above room temperature.[5–10] BFO has a rhombohedral *R*3*c* perovskite structure at room temperature and shows G-type antiferromagnetic order with a long-periodicity spiral below the Neel temperature of 643 K and ferroelectricity below 1103 K.[11] Although BFO thin films have these outstanding advantages, their high leakage currents, and weak spontaneous magnetization have been major obstacles for practical application in some devices.

Many efforts have been devoted recently to improving the multiferroic properties of BFO utilizing cation substitution to introduce chemical pressure into the system. Both Bi- and Fe-site substitution with a variety of cations have been attempted in BFO thin films and ceramics. For example, Ho, Ti, La, Co, and Dy doped BFO ceramics were synthesized to enhance the mutiferroicity.[12–14] Meanwhile, La, Mn, Ti, Cr, Mn, Co, Ni, and Cu doped BFO films were fabricated by pulsed laser deposition and chemical solution deposition on the $SrTiO_3$, GaAs, $LaAlO_3$, and Si substrates.[15–21] However, the improvement degree of multiferroic properties differs in each study even for the same additives. In addition, different orientational doped BFO thin films show great differences on the ferroelectric and ferromagnetic properties.[17] It is difficult to judge which additive is the most effective in improving the ferroelectric and ferromagnetic properties of BFO films. The multilayer structure consisting of doped BFO and other magneto-resistance materials[22,23] was found to be a promising way to simultaneously enhance the ferroelectric and ferromagnetic properties. In recent years, manganite films, such as $(La_{1-x}Sr_x)MnO_3$ (LSMO), have stimulated intense studies due to their colossal magnetoresistance (MR) effect[24] and rich physical phenomena, such as Jahn–Teller distortion,[25] metal–insulator transition,[26] phase separation,[24] etc. In the case of epitaxial BFO/LSMO heterostructures, the strain and interface effects between the BFO layer and the LSMO layer are induced, which influence their microstructure, electronic state, and magnetism.[27,28] A new ferromagnetic state was found because of the reconstruction of the electron orbit at the interface of the BFO/LSMO heterostructure.[29] Therefore, such an influence on the ferroelectric and ferromagnetic prop-

*Project supported by the National Natural Science Foundation of China (Grant No. 61078057), the Natural Science Foundation of Shannxi Province, China (Grant No. 2011GM6013), the Foundation for Fundamental Research of Northwestern Polytechnical University of China (Grant Nos. JC20110270 and 3102014JCQ01029), the Open Project of Key Laboratory for Magnetism and Magnetic Materials of Ministry of Education, Lanzhou University, China (Grant Nos. LZUMMM2013001 and LZUMMM2014007), and the Scholarship Fund of China (Grant No. 201303070058).

†Corresponding author. E-mail: zhaoch17@nwpu.edu.cn
‡Corresponding author. E-mail: xlin@nwpu.edu.cn

© 2014 Chinese Physical Society and IOP Publishing Ltd

erties of the doped BFO/LSMO heterostructure is probably related to an electronic orbit reconstruction at the interface and the complex interplay between orbit and spin degrees of freedom.

In the present work, the BBFO/LSMO heterostructures were fabricated by pulsed laser deposition. Detailed investigations on ferroelectric, ferromagnetic and leakage current properties have been performed and the results have been discussed. The interface effect of the BBFO/LSMO heterostructure was investigated with the aim of shedding more light on the relation between interface and multiferroic performance.

2. Experiment

The BBFO/LSMO heterostructures were deposited on $LaAlO_3$ (100) substrates by pulsed laser deposition. 10% Bi-enriched BBFO, 10% Bi-enriched BFO, and LSMO ceramic targets were synthesized via a solid-state reaction. In order to ensure the ideal stoichiometry of the targets, we prepared the targets with an excess of 6% of the mole of raw powder Bi_2O_3 to suppress the high volatility of Bi. After two sinterings, the compositions of the targets were analyzed quantitatively by using energy-dispersive spectrometry (EDS). Before the deposition, the substrates were treated by ultrasonic cleaning with acetone followed by ethanol, and finally dried by blowing pure nitrogen. The substrates were fixed in the substrate holder, and the distance between the targets and the substrates was 5 cm. Then, the chamber was evacuated below 10^{-6} Pa and the substrate was annealed at 750 °C for 30 min to clean the carbon contamination and form a high crystalline surface. A KrF excimer laser ($\lambda = 248$ nm) was used to ablate the target at a repetition rate of 2 Hz. The laser's energy density was about 2 J/cm^2. An LSMO layer was first deposited on the LAO(100) substrate at a substrate temperature of $\sim$ 750 °C, and the pressure of oxygen was 20 Pa. Subsequently, the BBFO was deposited on the LSMO layer at a substrate temperature of $\sim$ 600 °C, and the pressure of oxygen was 10 Pa. A polycrystalline BFO thin film was deposited on Pt/Ti/SiO_2/Si (100) under the same conditions for supplementary studies. All films were grown to a thickness of $\sim$ 160 nm to minimize the film thickness effects. After deposition, the as-grown thin films were *in situ* annealed at 600 °C and 1 atm pure oxygen for 30 min, and then gradually cooled down to room temperature.

The phase structures of the as-grown thin films were characterized by X-ray diffraction (XRD, Cu K_α radiation, D/max2200PC, Rigaku) using the θ –2θ scan mode. The valence states of Fe ions in BBFO were characterized with X-ray photoelectron spectroscopy (PHI-5400, PE). The microstructure, surface morphology, and piezoelectric properties of the sample were examined by atom force microscopy (AFM, Olympus, AC240TM, MFP-3D, Asylum Research) in tapping mode. To investigate the electrical properties of these films, circular Pt electrodes (diameter: 0.20 mm) were sputtered on the film surface using a shadow mask. Ferroelectric properties of the films were studied by using an RT6000VHS ferroelectric tester. The leakage currents of these films were measured by using a Keithley meter (Keithly 6517A). The magnetic properties of the thin films were characterized by a vibrating sample magnetometer (VSM, LakeShore 7400, Westerville, OH). All measurements were made at room temperature.

3. Results and discussion

Figure 1 shows the X-ray diffraction patterns of BBFO/LSMO heterostructure deposited on a $LaAlO_3$ substrate and randomly oriented BFO thin film deposited on a Pt/Ti/SiO_2/Si substrate. It is seen that the BBFO and LSMO thin films grew in a single phase perovskite structure with no detectable impurity or other phases. The peaks of BBFO and LSMO films merely appear on the (100) orientation from the LAO substrate, indicating that the films have a single (l00) orientation. Through analyzing the (200) peak, as shown in the inset of Fig. 1(a), the lattice constants of the BBFO and LSMO films were calculated to be 0.399 nm and 0.391 nm, respectively. The lattice constant of the BBFO is larger than that of bulk BFO. Therefore, the lattice distortion can be interpreted as a consequence of the compressive in-plane stress and C-oriented tensile stress[27] caused by the LSMO layer that has a smaller in-plane lattice parameter than that of BBFO.

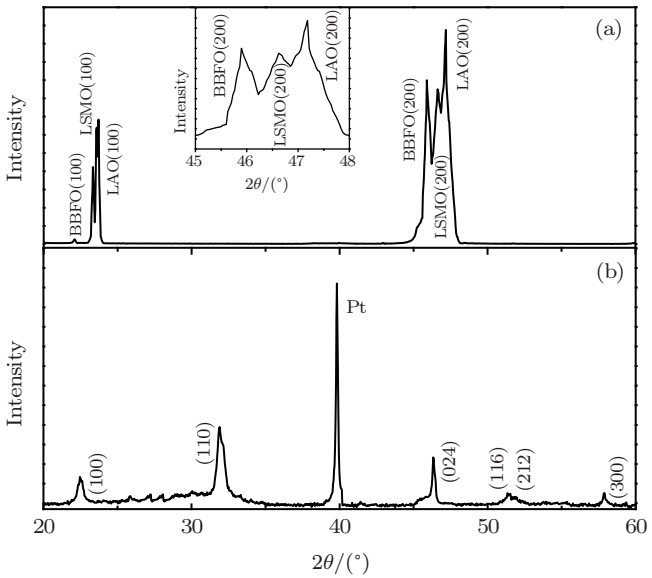


Fig. 1. (a) XRD patterns of BBFO/LSMO heterostructure grown on $LaAlO_3$ substrate, (b) XRD patterns of BFO thin film grown on Pt/Ti/SiO_2/Si substrate. The inset in (a) is a magnified XRD pattern of BBFO/LSMO heterostructure at the (200) peak position.

The ferroelectric properties of BBFO and BFO thin films were evaluated by a polarization-electric field (P–E) hysteresis loop, as shown in Fig. 2. It is difficult to obtain a saturated

P–E hysteresis loop for the BFO thin film due to a high leakage current in association with various defects. High leakage current in BFO thin film is primarily due to the occurrence of a small amount of Fe^{2+} ions, oxygen vacancies, and conductive Bi_2O_3 phase rather than the intrinsic property of BFO.[31] However, for epitaxial BBFO/LSMO heterostructure, a well-defined and rectangular $P-E$ loop was observed with a giant remanent polarization (P_r) of 85 μC/cm^2. The P_r value of the BBFO/LSMO heterostructure is quite comparable to that observed in $BiFeO_3$ single crystal ($P_r \sim 60$ μC/cm^2),[32] indicating the extremely high quality of our epitaxial BBFO thin film. Therefore, the enhancement in the remanent polarization could be attributed to several factors. (i) The suppression of Fe^{2+} ions could facilitate the formation of the lower leakage current density in a high electric field region, which is also largely responsible for the enhanced ferroelectric behavior. In order to determine the valency of the Fe element in BBFO thin film, the XPS energy spectrum of the Fe element in the BBFO/LSMO heterostructure is shown in Fig. 3. This is evidence that the Fe element in BBFO thin film is trivalent in contrast to the results of other researchers and the standard Fe_2O_3 XPS energy spectrum.[33,34] (ii) The Ba substitution for volatile Bi in BFO can suppress the formation of oxygen vacancies, which contributes to the decrease in leakage current density. Finally, the interface coupling between the BBFO layer and the LSMO layer should play an important role in the improvement of the ferroelectric behavior of the BFO/LSMO heterostructure. Consequently, the combined effects of these factors contribute to the enhancement of the ferroelectric property of the BBFO/LSMO heterostructure at room temperature.

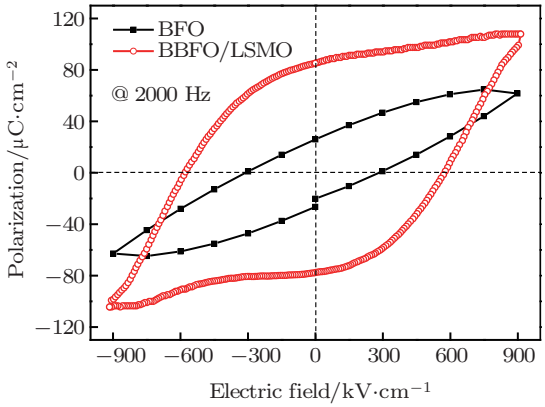


Fig. 2. (color online) *P–E* hysteresis loops of the BBFO/LSMO heterostructure and BFO thin film at 2000 Hz.

In order to better understand the reasons for the enhanced ferroelectricity, the leakage currents of BBFO and BFO thin films are shown in Fig. 4. It reveals that the BFO thin film deposited on the Pt/Ti/SiO_2/Si substrate exhibits a much higher leakage current than that of the BBFO thin film deposited on the $LaAlO_3$ with $La_{2/3}Sr_{1/3}MnO_3$ as the conductive buffer layer. This may be attributed to high densities of defects and oxygen vacancies and different electrode-film interfaces in the polycrystalline film as compared with epitaxial film.[17] It is confirmed that this heterostructure contributes to the decrease in leakage current density. It is well known that oxygen vacancies[35] are the most likely mobile charges, which often play an important role in the conduction of oxide ferroelectric thin films. Moreover, the ferroelectric domain wall morphology of epitaxial BBFO thin film also seriously affects the magnitude of the leakage current.

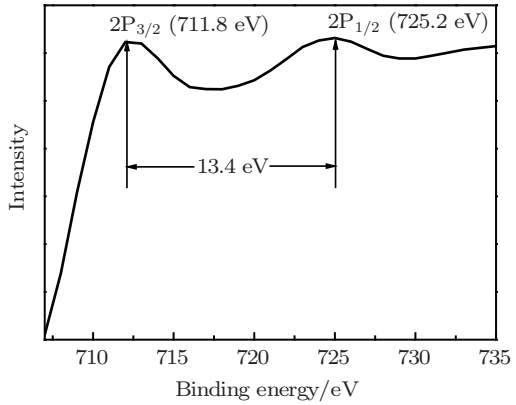


Fig. 3. XPS energy spectrum of the Fe element in the BBFO/LSMO heterostructure.

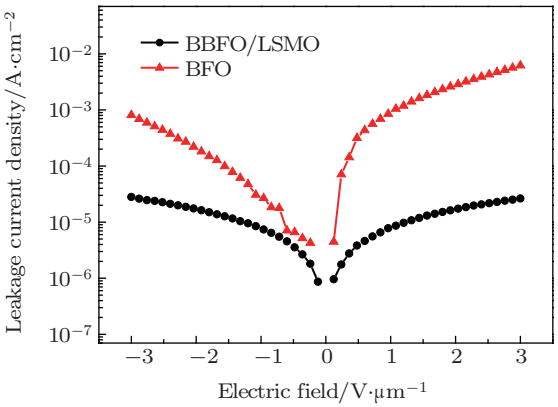


Fig. 4. (color online) Leakage current density as a function of the electric field for BBFO and BFO thin films.

The out-of-plane domain structure of BBFO thin film is shown in Fig. 5(a). Figure 5(b) is the surface morphology image corresponding to the region shown in Fig. 5(a) for its domain image, revealing a flat surface and uniform distribution of grains. The RMS roughness was 2.082 nm over a 1 μm^2 area, and the average grain size is less than 100 nm. The ferroelectric domain walls are fairly consistent with the grain boundaries (see the marks in Fig. 5). It is shown that the BBFO thin film exhibits a mixed mosaic and stripe-like domain structure. It is well known that this stripe-like structure corresponds to arrays of 71° domain walls, while the mosaic structure is comprised of a mixture of all possible domain wall types, particularly, large fractions of 109° domain walls and smaller fractions of 71° and 180° walls.[36] It has been

reported that 109° and 180° domains have a much larger electrostatic potential step and hence larger conductivity than 71° domains.[37] Consequently, it is plausible that BBFO thin film demonstrates a relatively low leakage current density because of the mixed domain structure. Therefore, the interface of the BBFO/LSMO heterostructure significantly influences the ferroelectric domains structure of BBFO thin film and hence a lower leakage current density, which determine the ferroelectric properties of BBFO thin film.

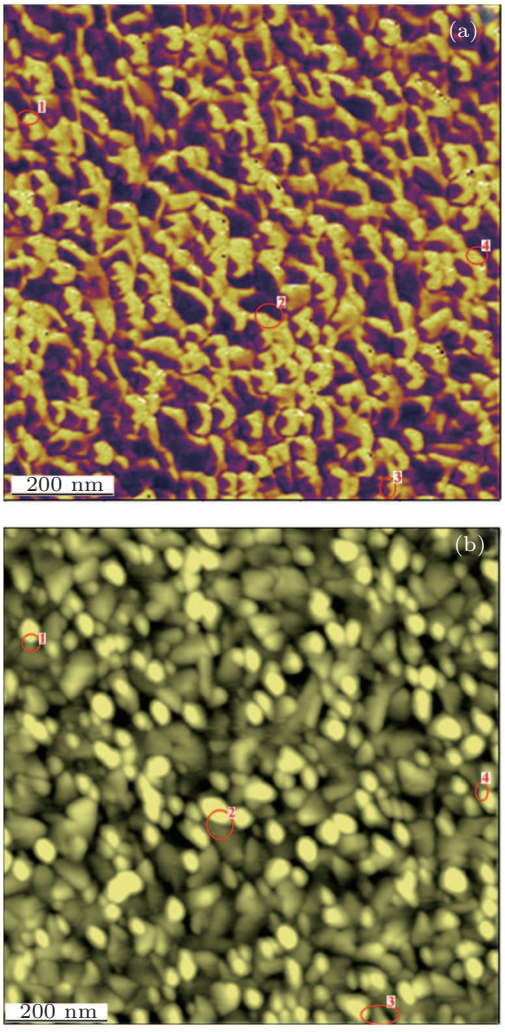


Fig. 5. (color online) (a) A PFM image of BBFO thin film and (b) the corresponding AFM image.

Figure 6 shows the magnetization characteristics of the BBFO/LSMO heterostructure and BFO thin film measured at a maximum magnetic field of 6000 Oe applied parallel to the substrate surface at room temperature. Before magnetic measurement, the magnetic properties of two kinds of substrates and $La_{2/3}Sr_{1/3}MnO_3$ thin film were measured and the results demonstrate that the contribution of these components to the magnetic performance of the as-deposited thin films is very limited and can be ignored. The saturated magnetization M_s ($\sim$12.4 emu/cm^3) for the BBFO/LSMO heterostructure is enhanced dramatically compared with BFO thin film grown on the Pt/Ti/SiO_2/Si substrate, which is much larger than that of the pure BFO thin films previously reported.[38] There are several possible considerations that are responsible for the observed magnetization in the BBFO/LSMO heterostructure: one possible source is the contribution of the LSMO layer. However, the resistance-temperature curve (inset (b) of Fig. 6) shows that there is a metal-to-insulator transition at 275 K, which demonstrates the LSMO thin film is paramagnetic[25] at room temperature. Meanwhile, the magnetic measurement (inset (a) of Fig. 6) demonstrates the magnetic performance of the LSMO thin film is very limited and can be ignored. The results confirm that the LSMO layer has made very little contribution to the magnetic property of the BBFO/LSMO heterostructure. A second possibility is that the increase of magnetic property for the BBFO/LSMO heterostructure is attributed to the formation of excessive Fe^{2+}. However, the XPS energy spectrum of the Fe element in the BBFO/LSMO heterostructure is evidence that the Fe element in BBFO thin film is trivalent, as shown in Fig. 3. Therefore, the enhancement of magnetization has nothing to do with the formation of Fe^{2+} ions in this work. Furthermore, the enhancement of magnetization is presumably a consequence of the interface effect. On one hand, according to the Goodenough–Kanamori–Anderson rule,[39–41] super-exchange interactions between Fe^{3+} and Mn^{3+}, Fe^{3+} and Mn^{4+} are ferromagnetic coupling, resulting in the enhancement of magnetization. On the other hand, the reconstruction of the electron orbit at the interface of the heterostructure elicits a new ferromagnetic state.[32] It is believed that the interface effect is the critical factor that results in the enhancement of magnetization of the BBFO/LSMO heterostructure.

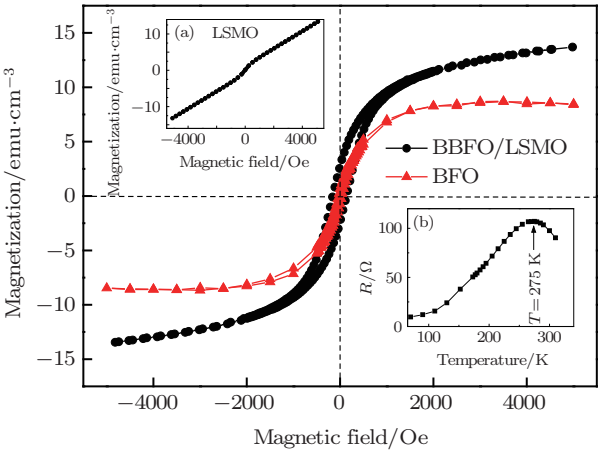


Fig. 6. (color online) Magnetic hysteresis loops of BBFO and BFO thin films. Inset (a): magnetic hysteresis loops of the LSMO thin film; inset (b): resistance–temperature curve of the LSMO thin film.

4. Conclusion

In summary, this study investigated the multiferroic properties of the BBFO/LSMO heterostructure, which was epitaxially grown on a single-crystal LAO substrate by pulsed laser

deposition. The interface coupling effect plays an important role in the enhancement of the ferroelectric polarization and magnetic behavior. In the BBFO/LSMO heterostructure, a high P_r value of ~ 85 μC/cm^2 was achieved, and a good magnetic behavior was observed at room temperature. In addition, the structures of the ferroelectric domains are also responsible for the lower leakage current and good ferroelectric polarization behavior.

References

[1] Ramesh R and Spaldin N A 2007 *Nat. Mater.* **6** 21
[2] Catalan G and Scott J F 2009 *Adv. Mater.* **21** 2463
[3] Wang J, Neaton J B, Zheng H, Nagarajan V, Ogale S B, Liu B, Viehland D, Vaithyanathan V, Schlom D G, Waghmare U V, Spaldin N A, Rabe K M, Wuttig M and Ramesh R 2003 *Science* **299** 1719
[4] Eerenstein W, Mathur N D and Scott J F 2006 *Nature* **442** 7104
[5] Spaldin N A and Fiebig M 2005 *Science* **309** 391
[6] Li J F, Wang J L, Wuttig M, Ramesh R, Wang N, Ruette B, Pyatakov A P, Zvezdin A K and Viehland D 2004 *Appl. Phys. Lett.* **84** 5261
[7] Palai R, Katiyar R S, Schmid H, Tissot P, Clark S J, Robertson J, Redfern S A, Catalan G and Scott J F 2008 *Phys. Rev. B* **77** 014110
[8] Scott J F, Palai R, Kumar A, Singh M K, Murari N, Karan N K and Katiyar R S 2008 *J. Am. Ceram. Soc.* **91** 1762
[9] Wu J G and Wang J 2010 *Acta Mater.* **58** 1688
[10] Neaton J B, Ederer C, Waghmare U V, Spaldin N A and Rabe K M 2005 *Phys. Rev. B* **71** 014113
[11] Wang K F, Liu J M and Ren Z F 2009 *Adv. Phys.* **58** 321
[12] Lin P T, Li X, Zhang L, Yin J H, Cheng X W, Wang Z H, Wu Y C and Wu G H 2014 *Chin. Phys. B* **23** 047701
[13] Gu Y H, Liu Y, Yao C, Ma Y W, Wang Y, Chan H L W and Chen W P 2014 *Chin. Phys. B* **23** 037501
[14] Song G L, Luo Y P, Su J, Zhou X H and Chang F G 2013 *Acta Phys. Sin.* **62** 097502 (in Chinese)
[15] Gao G Y, Yang Z B, Huang W, Zeng H Z, Wang Y, Chan H L W, Wu W B and Hao J H 2013 *J. Appl. Phys.* **114** 094106
[16] Wang D Y, Ding R and Li S 2013 *J. Am. Ceram. Soc.* **96** 2531
[17] Wang D Y, Chan N Y, Zheng R K, Kong C, Lin D M, Dai J Y, Chan H L W and Li S 2011 *J. Appl. Phys.* **109** 114105
[18] Ahmed M A, Mansour S F and Afifi M 2013 *J. Alloys Comp.* **578** 303
[19] Naganuma H, Miura J and Okamura S 2008 *Appl. Phys. Lett.* **93** 052901
[20] Luo L R, Shen K, Xu Q Y, Zhou Q, Wei W and Gondal M A 2013 *J. Alloys Comp.* **558** 73
[21] Hu Z Q, Li M Y, Liu J, Pei L, Wang J, Yu B F and Zhao X Z 2010 *J. Am. Ceram. Soc.* **93** 2743
[22] Allibe J, Infante I C, Fusil S, Bouzehouane K, Jacquet E, Deranlot C, Bibes M and Barth'el'emy A 2009 *Appl. Phys. Lett.* **95** 182503
[23] Ke Q Q, Lu W L, Huang X L and Wang J 2012 *J. Electrochem. Society* **159** G11
[24] Dagotto E, Hotta T and Moreo A 2001 *Phys. Rep.* **344** 1
[25] Ziese M 2002 *Rep. Prog. Phys.* **65** 143
[26] Imada M, Fujimori A and Tokura Y 1998 *Rev. Mod. Phys.* **70** 1039
[27] Rao S S, Prater J T, Wu F, Shelton C T, Maria J P and Narayan J 2013 *Nano Lett.* **13** 5814
[28] Liu G Z, Wang C, Wang C C, Qiu J, He M, Xing J, Jin K J, Lu H B and Yang G Z 2008 *Appl. Phys. Lett.* **92** 122903
[29] Yu P, Lee J S, Okamoto S, Rossell M D, Huijben M, Yang C H, He Q, Zhang J X, Yang S Y, Lee M J, Ramasse Q M, Erni R, Chu Y H, Arena D A, Kao C C, Martin L W and Ramesh R 2010 *Phys. Rev. Lett.* **105** 027201
[30] Chu Y H, Martin L W, Holcomb M B and Ramesh R 2007 *Mater. Today* **10** 16
[31] Clark S J and Robertson J 2007 *Appl. Phys. Lett.* **90** 132903
[32] Lebeugle D, Colson D, Forget A and Viret M 2007 *Appl. Phys. Lett.* **91** 022907
[33] Yamashita T and Hayes P 2008 *Appl. Surf. Sci.* **254** 2441
[34] Luo W B, Zhu J, Li Y R, Wang X P, Zhao D, Xiong J and Zhang Y 2007 *Appl. Phys. Lett.* **91** 082501
[35] Yan J, Hu G D, Chen X M, Wu W B and Yang C H 2008 *J. Appl. Phys.* **104** 076103
[36] Zavaliche F, Yang S Y, Zhao T, Chu Y H, Cruz M P, Eom C B and Ramesh R 2006 *Phase Trans.* **79** 991
[37] Seidel J, Martin L W, He Q, Zhan Q, Chu Y H, Rother A, Hawkridge M E, Maksymovych P, Yu P, Gajek M, Balke N, Kalinin S V, Gemming S, Wang F, Catalan G, Scott J F, Spaldin N A, Orenstein J and Ramesh R 2009 *Nat. Mater.* **8** 229
[38] EerenStein W, Morrison F D, Dho J, Blamire M G, Scott J F and Mathur N D 2005 *Science* **307** 1203a
[39] Anderson P W 1950 *Phys. Rev.* **79** 350
[40] Goodenough J B 1955 *Phys. Rev.* **100** 564
[41] Kanamori J 1959 *J. Phys. Chem. Solids* **10** 87